

# PCCP

Accepted Manuscript



This is an *Accepted Manuscript*, which has been through the Royal Society of Chemistry peer review process and has been accepted for publication.

*Accepted Manuscripts* are published online shortly after acceptance, before technical editing, formatting and proof reading. Using this free service, authors can make their results available to the community, in citable form, before we publish the edited article. We will replace this *Accepted Manuscript* with the edited and formatted *Advance Article* as soon as it is available.

You can find more information about *Accepted Manuscripts* in the [Information for Authors](#).

Please note that technical editing may introduce minor changes to the text and/or graphics, which may alter content. The journal's standard [Terms & Conditions](#) and the [Ethical guidelines](#) still apply. In no event shall the Royal Society of Chemistry be held responsible for any errors or omissions in this *Accepted Manuscript* or any consequences arising from the use of any information it contains.

## Analyzing Torquoselectivity in Electrocyclic Ring Opening Reactions of *trans*-3,4-Dimethylcyclobutene and 3-Formylcyclobutene through Electronic Structure Principles

Alejandro Morales-Bayuelo<sup>\*1</sup>, Sudip Pan<sup>2</sup>, Julio Caballero<sup>1</sup>, and Pratim K. Chattaraj<sup>\*2</sup>

<sup>1</sup>*Centro de Bioinformática y Simulación Molecular (CBSM), Universidad de Talca, 2 Norte 685, Casilla 721, Talca, Chile*

<sup>2</sup>*Department of Chemistry and Center for Theoretical Studies*

*Indian Institute of Technology Kharagpur, 721302, India*

\*E-mails of corresponding authors: [alejandr.morales@uandresbello.edu](mailto:alejandr.morales@uandresbello.edu);  
[pkc@chem.iitkgp.ernet.in](mailto:pkc@chem.iitkgp.ernet.in)

---

**Abstract:** The validity of the maximum hardness, minimum electrophilicity and minimum polarizability principles is assessed to explain the phenomenon of the torquoselectivity (inward and outward preference) in the conrotatory ring opening reactions of *trans*-3,4-dimethylcyclobutene into Z,Z- and E,E-butadienes and 3-formylcyclobutene into E- and Z-2,4-pentadienals. The hardness, average polarizability and electrophilicity profiles are computed along the intrinsic reaction coordinate and divided into three relevant stages. The transition states involved in the unfavorable inward conrotation of *trans*-3,4-dimethylcyclobutene and in the unfavorable outward conrotation of 3-formylcyclobutene are found to be higher in energy, softer, more electrophilic and more polarizable than the transition states corresponding to the torquoselective outward and inward conrotations, respectively. These observations are in conformity with the maximum hardness, minimum electrophilicity and minimum polarizability principles. The sharp changes in the local reactivity descriptors are also observed around the transition states in their respective profiles.

---

## Introduction

In literature, various qualitative chemical concepts like electronegativity<sup>1</sup> ( $\chi$ ), polarizability<sup>2</sup> ( $\alpha$ ), hardness<sup>3</sup> ( $\eta$ ), electrophilicity<sup>4,5</sup> ( $\omega$ ), etc. became very popular in describing several reactivity and bonding features associated with atoms and molecules. The maximum hardness principle (MHP) was introduced by Pearson<sup>6</sup> as “there seems to be a rule of nature that molecules arrange themselves so as to be as hard as possible” which was later provided with a formal proof by Parr and Chattaraj<sup>7</sup> under the conditions of constant chemical potential ( $\mu$ ) and external potential ( $v(\mathbf{r})$ ). The minimum hardness value attained by a transition state (TS) was also later put forward as a corollary to MHP.<sup>8</sup>

Minimum electrophilicity principle<sup>9-11</sup> (MEP) is another electronic structure principle, which is originated from an extension of MHP. It was known that during chemical reactions, molecular vibration and internal rotations, the extrema in  $\omega$  take place at points where:

$$\frac{\partial \omega}{\partial y} = \frac{\mu}{\eta} \left( \frac{\partial \mu}{\partial y} \right) - \frac{1}{2} \left( \frac{\mu}{\eta} \right)^2 \left( \frac{\partial \eta}{\partial y} \right) \quad (1)$$

Here,  $y$  is a reaction coordinate or bond length, or bond angle or dihedral angle in the process of chemical reaction or stretching, or bending or internal rotation, respectively. Due to the convexity of the energy,  $\mu$  is always negative ( $\mu < 0$ ) and  $\eta$  is always positive ( $\eta > 0$ ),<sup>12</sup> therefore  $\omega$  has an extremum when the slopes of the changes in  $\mu$  and  $\omega$  are opposite in signs. In other words,  $\omega$  has a minimum (maximum) value when  $\mu$  and  $\eta$  have maximum (minimum) values for a given  $y$ . Therefore, validity of MHP implies that  $\eta$  has a maximum value for the reactant, product or an intermediate and a minimum value at the TSs, which further dictates that  $\omega$  should have a minimum value for the reactant/product/intermediate and a maximum value at the TSs.

Taking into account the inverse relationship between  $\eta$  and  $\alpha$ , ( $\eta \propto 1/\alpha^{1/3}$ ), a minimum polarizability principle<sup>13</sup> (MPP) was proposed. It states that “the natural direction of evolution of any system is towards a state of minimum polarizability”.

These electronic structure principles were found to be valid in many cases like internal rotations, molecular vibrations, atomic shell structure, isomer stability, chemical reactions,

aromaticity, electronic excitations, stability of magic clusters, time dependent situations, Woodward-Hoffmann rules, chaotic ionizations, and a number of other categories of chemical processes. In fact, most of the non-totally symmetric vibrations obey MHP well due to the near constant value of chemical potential and external potential during nuclear displacements. However, certain vibrations and chemical processes were also reported to disobey these principles. In general, though the validity of these principles was not met for certain situations, these principles can provide important information about many chemical processes and even to discern the preference of a path over another in a given reaction.<sup>14</sup>

Several pericyclic reaction were studied<sup>15</sup> to assess the applicability of electronic structure principles towards prediction of Woodward-Hoffmann rules and it was concluded that these principles are consistent with the predictions of the Woodward-Hoffmann rules on transition states (TSs) associated with the symmetry-forbidden disrotation and symmetry-allowed conrotation. The whole analysis was based on electron density bypassing the orbitals.

In the present study, with an aim to extrapolate these findings, we have studied the validity of these electronic structure principles (MHP, MEP and MPP) in the torquoselectivity of *trans*-3,4-dimethylcyclobutene and 3-formylcyclobutene. Since the concept of torquoselectivity was introduced by Houk in the electrocyclic reactions,<sup>16,17</sup> many studies have been undertaken from the theoretical and experimental points of view.<sup>18-29</sup> The torquoselectivity<sup>24</sup> is defined as “*the preference for inward or outward rotation of substituents in conrotatory or disrotatory electrocyclic reactions*”. In this sense, the torquoselectivity is a secondary effect in the Woodward-Hoffmann rules defining the special orientation to the inward or outward preference in the ring opening of electrocyclic reactions. While the outward conrotation was found to be more preferable than that of the inward conrotation in case of *trans*-3,4-dimethylcyclobutene,<sup>17</sup> the reverse is true for the case of 3-formylcyclobutene.<sup>30-33</sup> It cannot be explained solely by the conventional steric effects present therein and the analysis of the unfavorable closed-shell repulsion may become important. Houk and co-workers<sup>13,30-33</sup> explained these observations through electronic effects and the nature of interaction between frontier molecular orbitals during conrotation. In case of *trans*-3,4-dimethylcyclobutene, while upon inward rotation the filled substituent donor orbitals get overlapped with the highest occupied molecular orbital (HOMO) of

the transition state resulting in a destabilizing cyclic four-electron interaction, in outward conrotation substituent donor orbitals overlap with the lowest unoccupied molecular orbital (LUMO) of the transition state providing stability. On the other hand, in case of 3-formylcyclobutene the low lying substituent vacant orbital interacts with the HOMO of the transition state resulting in stabilizing two-electron interaction in inward rotation. Conversely, such type of stabilization is small in the outward rotation.

We have chosen the thermal isomerization reactions of *trans*-3,4-dimethylcyclobutene and 3-formylcyclobutene through two conrotatory reaction pathways (inward and outward) for the current study to establish that one can predict the torquoselectivity from the electronic structure principles (MHP, MEP and MPP) without any prior knowledge about the frontier molecular orbitals and energy and accordingly this study will be complementary to the elegant approach towards analyzing torquoselectivity as prescribed by Houk and coworkers.<sup>16-18,30-33</sup> In addition, the present study is an attempt to demonstrate the validity of the MHP, MEP and MPP in the torquoselectivity of electrocyclic reactions using the above mentioned case studies. The thermochemical analysis and the electronic nature associated with the breaking and bonding processes of *trans*-3,4-dimethylcyclobutene were reported previously.<sup>34</sup>

### Computational Details

The geometry optimizations of all the studied structures were carried out at the B3LYP/6-31G(d,p) level<sup>35,36</sup> using GAUSSIAN 09 program package.<sup>37</sup> The transition states were verified by the presence of only one imaginary frequency corresponding to the desired mode. The intrinsic reaction coordinate (IRC) paths were also computed to verify that the transition states are indeed connected properly with the reactants and reaction products. The information about the energies of frontier molecular orbitals was obtained by single point energy computation at each point of IRC at the B3LYP/6-31G(d,p) level.

Conceptual density functional theory (CDFT)<sup>5,38-40</sup> based global reactivity descriptors like  $\chi^1$ ,  $\eta^3$  and  $\omega^4$ ,<sup>5</sup> and local reactivity descriptors like condensed-to-atom Fukui function<sup>41,42</sup> ( $f_k^x$ ) and local philicity<sup>43,44</sup> ( $\omega_k^x$ ) were calculated as follows:

For an N-electron system having total energy  $E$ ,  $\chi$  and  $\eta$  can be defined as

$$\chi = - \left( \frac{\partial E}{\partial N} \right)_{v(\mathbf{r})} = -\mu \quad (2)$$

$$\eta = \left( \frac{\partial^2 E}{\partial N^2} \right)_{v(\mathbf{r})} \quad (3)$$

where  $v(\mathbf{r})$  and  $\mu$  are external and chemical potentials, respectively.  $\omega$  is defined as

$$\omega = \frac{\mu^2}{2\eta} = \frac{\chi^2}{2\eta} \quad (4)$$

Applying the finite difference approximations to equations 2 and 3,  $\chi$  and  $\eta$  can be expressed as

$$\chi = \frac{I + A}{2} \quad (5)$$

and

$$\eta = I - A \quad (6)$$

where  $I$  and  $A$  are the ionization potential and electron affinity, respectively.

Here  $I$  and  $A$  were computed by applying Koopmans' theorem.

$$\text{Hence, } I = -E_{\text{HOMO}} \quad (7)$$

$$\text{and } A = -E_{\text{LUMO}} \quad (8)$$

On the other hand, the  $\alpha^2$  is a second order derivative of energy with respect to the applied homogeneous electric field and can be computed as

$$\alpha = \frac{1}{3} (\alpha_{xx} + \alpha_{yy} + \alpha_{zz}) \quad (9)$$

$f_k^x$  ( $x = +, -$ ) could be computed as:

$$f_k^+ = q_k(N+1) - q_k(N) \text{ for nucleophilic attack} \quad (10a)$$

$$f_k^- = q_k(N) - q_k(N-1) \text{ for electrophilic attack} \quad (10b)$$

where  $q_k$  refers to the electron population at  $k^{\text{th}}$  atomic site in a molecule. Here, we adopted natural population analysis (NPA) scheme to evaluate atomic charge.

$\omega_k^x$  ( $x = +, -$ ) could be computed as

$$\begin{aligned} \omega^x(\mathbf{r}) &= \omega \cdot f^x(\mathbf{r}) \\ \text{or, } \omega_k^x &= \omega \cdot f_k^x \end{aligned} \quad (11)$$

+ and – signs represent nucleophilic and electrophilic attacks, respectively.

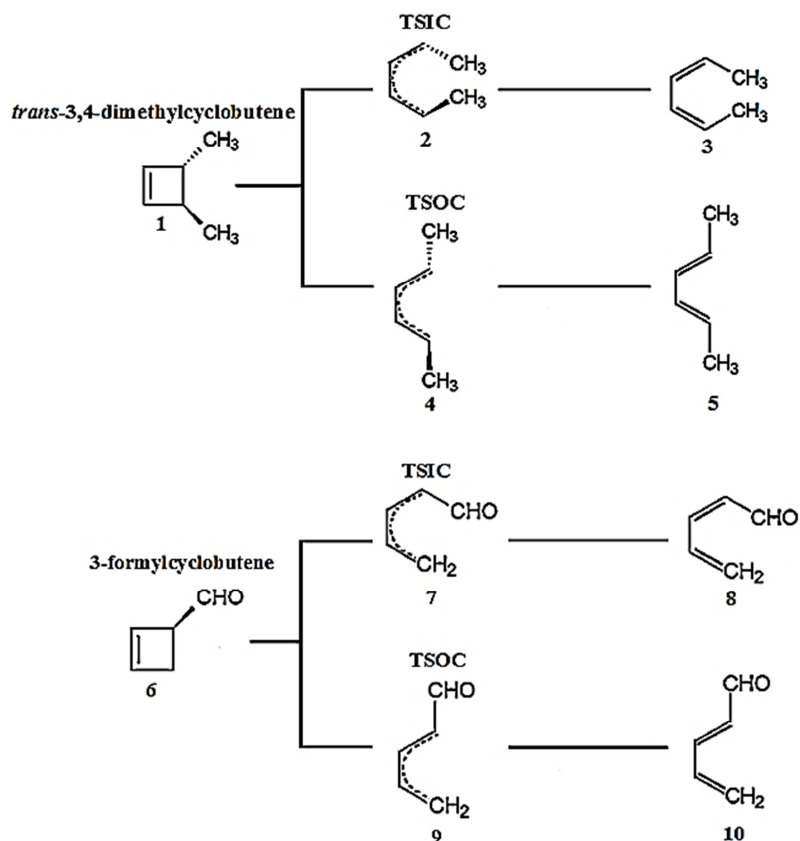
The reaction electronic flux (REF,  $J(\xi)$ ) corresponding to a chemical process along IRC ( $\xi$ ) is defined as:<sup>45</sup>

$$J(\xi) = -\frac{d\mu}{d\xi} \quad (12)$$

REF describes the electronic activity occurring along the IRC. While positive values of  $J(\xi)$  show spontaneous changes in the electronic density, analogous to the bond formation or bond strengthening, negative values represent non-spontaneous electronic reordering similar to the bond breaking or bond weakening.

## Results and Discussion

A pictorial depiction of the process studied here is presented in Scheme 1 in which *trans*-3,4-dimethylcyclobutene (**1**) and 3-formylcyclobutene (**6**) undergo electrocyclic ring opening reaction under thermal condition via inward and outward conrotation producing Z,Z- and E,E-butadienes (**3** and **5**) and Z- and E-2,4-pentadienals (**8** and **10**), respectively.



**Scheme 1.** Reactant, transition states and products involved in the electrocyclic ring opening reactions of *trans*-3,4-dimethylcyclobutene and 3-formylcyclobutene.

The TSs associated with the ring opening of **1** and **6** in outward conrotatory (TSOC) and inward conrotatory (TSIC) fashions along with the geometrical parameters are displayed in Figure 1. In the corresponding TSs, the bond lengths of the bond broken (C2-C5) in the TSOC are somewhat smaller than that in the TSIC. On the other hand, the (C1) and (C6) carbon atoms in case of **1** and the (C1) and (C5) carbon atoms in **6** are much closer in the TSIC than those in the respective TSOC structures.

Here, we have scrutinized these two reaction paths, inward and outward conrotation in order to analyze the torquoselectivity from the different CDFT based reactivity descriptors in conjunction with the electronic structure principles without any prior knowledge of the favorable/unfavorable interaction between the frontier molecular orbitals.

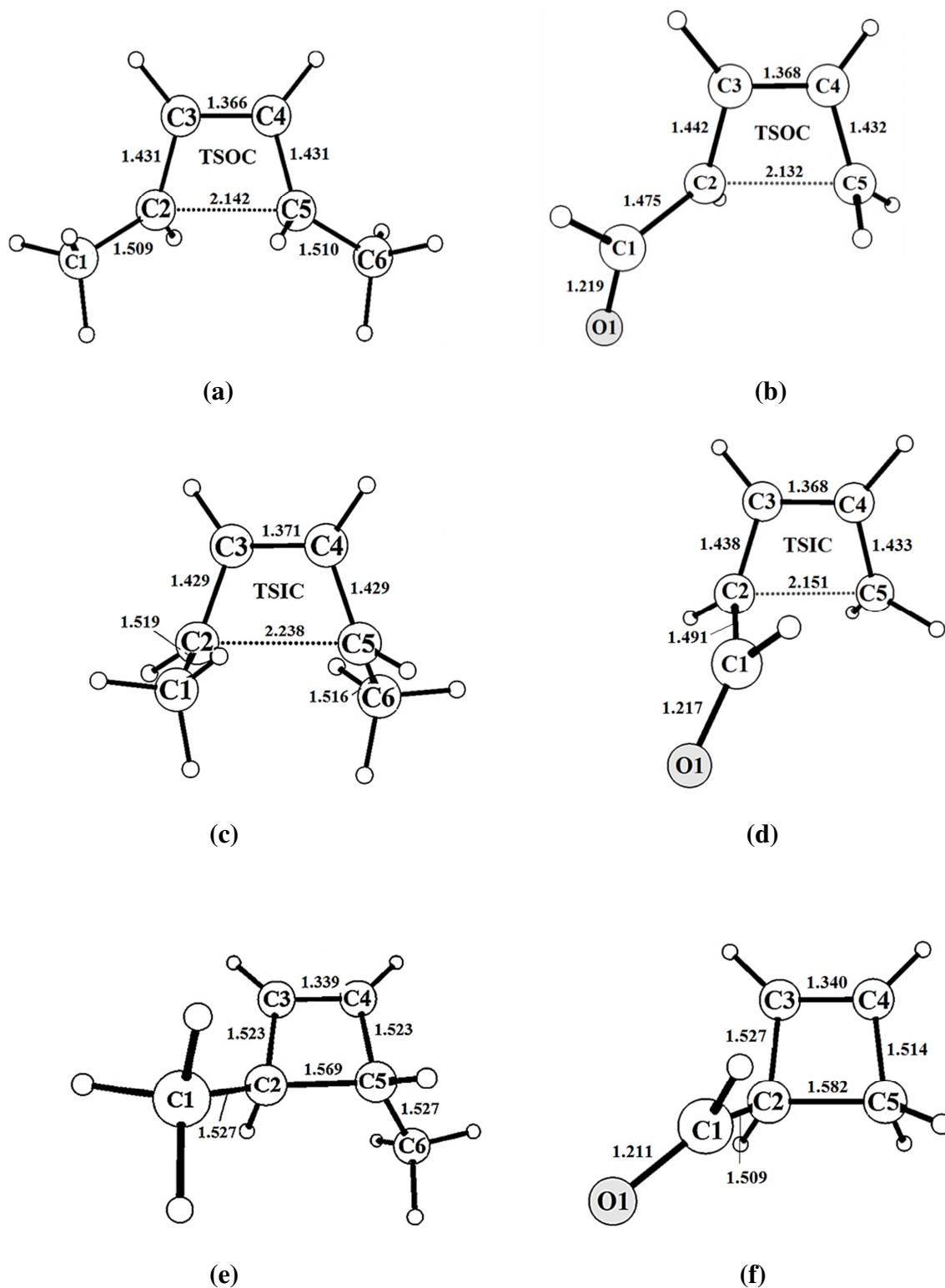


**Figure 1.** Various bond lengths (in Å) of the transition state outward conrotatory (TSOC) (a, b), the transition state inward conrotatory (TSIC) (c, d), and ground state minimum energy

geometries (**e**, **f**) of *trans*-3,4-dimethylcyclobutene and 3-formylcyclobutene at the B3LYP/6-31G(d,p) level.

First, we have divided the reaction path into three stages relevant to the corresponding molecular rearrangements. The REF is a very useful descriptor to follow the change in electronic activity during the course of a reaction process. Stage I represents the reactants before the TS whereas stage II corresponds to the TSs and finally another stage describes the appearance of the reaction product (stage III). The plots of REF along the IRC for the two processes involving TSIC and TSOC are provided in Figure 2. For both the cases, REF varies very little at the beginning and then it starts to decrease. After attaining a minimum, it increases steeply to get a maximum and then it reduces gradually to become zero in the final product region.

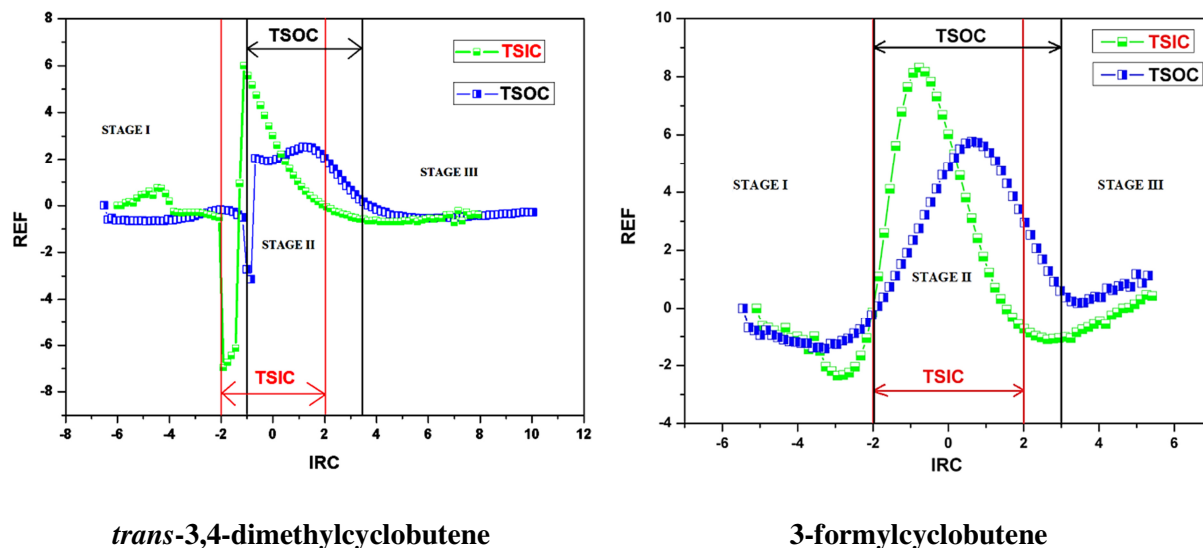


**Figure 2.** The reaction electronic flux (REF in kcal.mol<sup>-1</sup>.ξ<sup>-1</sup>) profiles along IRC (ξ, amu<sup>1/2</sup>bohr) of ring opening processes of *trans*-3,4-dimethylcyclobutene and 3-formylcyclobutene.

The negative REF value indicates the bond breaking of C2-C5 bond and after breaking of this bond, the C2-C3 and C5-C4 bonds gradually get a double bond character with a decrease in their respective bond lengths. This is indicated by the positive REF value in the plot. Therefore, in case of **1** the bond breaking and bond strengthening phenomenon occurs at ξ ≈ -2 to +2 amu<sup>1/2</sup>bohr for TSIC and at ξ ≈ -1 to +3.5 amu<sup>1/2</sup>bohr for TSOC whereas the same occurs at ξ ≈ -2 to +2 amu<sup>1/2</sup>bohr for TSIC and at ξ ≈ -2 to +3 amu<sup>1/2</sup>bohr for TSOC in case of **6**. These regions

could be treated as the stage II phases for the respective processes. According to the generalized transition state theory,<sup>46,47</sup> a transition state is not located exactly at the saddle point, rather it is placed in a region separated by two parallel dividing surfaces. In fact, this is the basis of the transition state spectroscopy<sup>48,49</sup> in which TS is considered as a region involving all the states of the systems from perturbed reactants to products. Therefore, in our cases, the above mentioned regions could be treated as TSs. It may also be noted that the change in electronic activity occurring in TSIC path is larger than that in the TSOC path.

Variation of relative energy along the IRC is displayed in Figure 3. As expected from the larger crowding in TSIC in **1**, in stage II the energy of the reaction path involving TSIC rises much steeply compared to that involving TSOC.

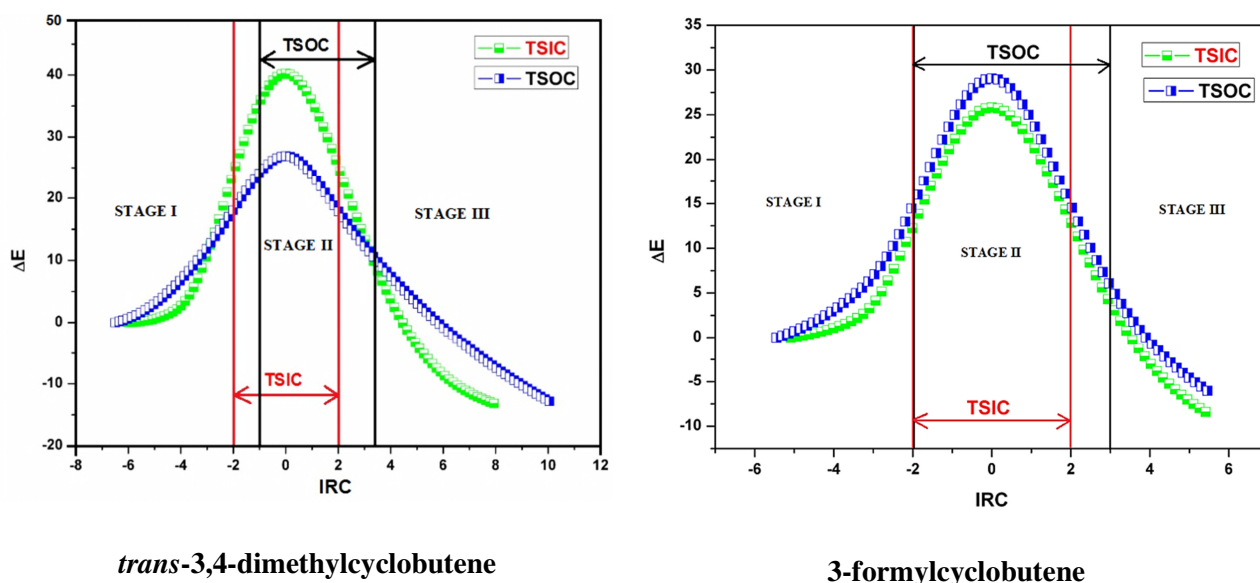


**Figure 3.** Variation of relative energy ( $\Delta E$ , kcal/mol) along IRC ( $\xi$ ,  $\text{amu}^{1/2}\text{bohr}$ ) for the electrocyclic ring opening process of *trans*-3,4-dimethylcyclobutene and 3-formylcyclobutene at the B3LYP/6-31G(d,p) level.

The inward conrotation also goes via larger activation energy barrier than that of the outward conrotation. The TSIC is found to be 11.3 kcal/mol higher in energy than the TSOC. In the stage III involving energy relaxation, though TSIC path decreases more steeply, the product corresponding to the TSOC path is 3.1 kcal/mol more stable than that of the TSIC path. Therefore, the product through TSOC path would be both kinetically and thermodynamically

controlled. On the other hand, in case of **6** the reaction path involving TSIC proceeds through the lower barrier by 4.0 kcal/mol than that one involving TSOC. Similarly the product belonging to the TSIC path is more stable by 3.2 kcal/mol than that of the TSOC path.

Now, from the MHP, MEP and MPP, we may expect that the TS associated with the torquoselective conrotation (outward in **1** and inward in **6**) would be harder, less electrophilic and less polarizable than that of the TS associated with forbidden conrotation (inward in **1** and outward in **6**). In addition, the TSs should go through a minimum in  $\eta$  and maxima in  $\omega$  and  $\alpha$  in their respective profiles according to the associated electronic structure principles. We are interested in the stage II where the TSs lie.

The  $\eta$  profile along the IRC is provided in Figure 4. In case of **1**, in TSIC path the  $\eta$  value decreases sharply from around  $\xi \approx -2$  amu<sup>1/2</sup>bohr and then it reaches a minimum at around  $\xi \approx +1$  amu<sup>1/2</sup>bohr. Afterwards it increases rapidly as it enters in the product formation zone.

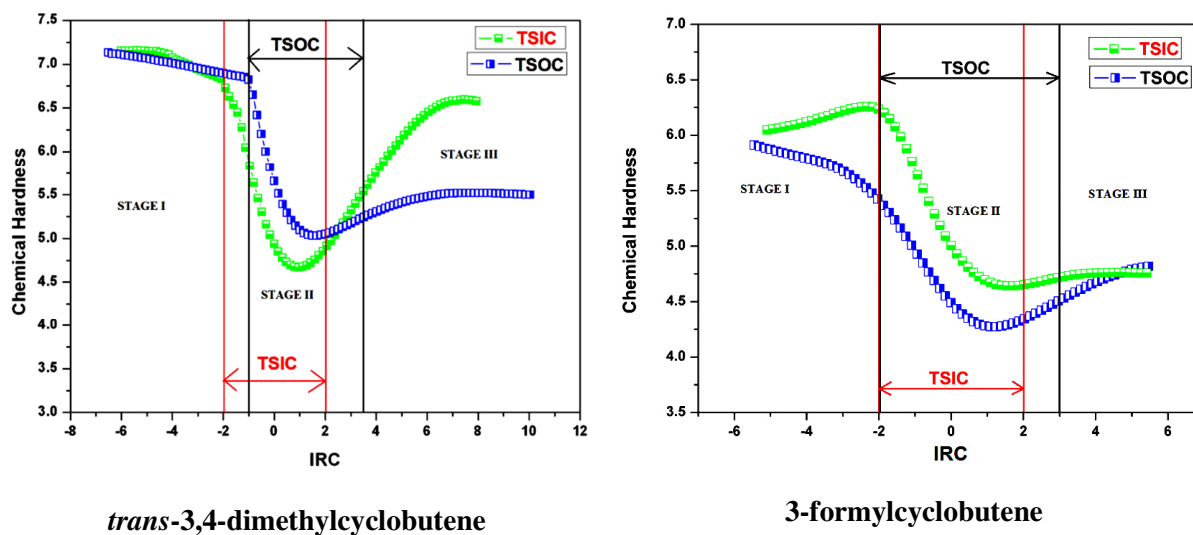


**Figure 4.** Chemical hardness ( $\eta$ , eV) profiles along IRC ( $\xi$ , amu<sup>1/2</sup>bohr) at the B3LYP/6-31G(d,p) level.

Therefore, minimum in the  $\eta$  profile resides perfectly within the stage II region, thereby perfectly obeying the MHP dictating a minimum  $\eta$  value at TS. Similarly, in case of TSOC path the  $\eta$  value decreases very rapidly from  $\xi \approx -1$  amu<sup>1/2</sup>bohr to reach a minimum around at  $\xi \approx +1.5$  amu<sup>1/2</sup>bohr. Hence, in this case also the minimum in the  $\eta$  profile occurs within stage II region. On the other hand, in case of **6** in both TSOC and TSIC paths,  $\eta$  value tends to decrease

sharply around from  $\xi \approx -2 \text{ amu}^{1/2}\text{bohr}$  and thereafter attains a minimum value at  $1.5 \text{ amu}^{1/2}\text{bohr}$  for TSIC and  $1.1 \text{ amu}^{1/2}\text{bohr}$  for TSOC path. Hence, they also follow MHP. It may also be noted that the favorable TSOC in **1** and favorable TSIC in **6** are harder than the respective unfavorable transition states throughout the stage II. So, MHP is perfectly obeyed during the course of the stage II.

Now, let us look at the  $\omega$  profile along IRC to assess the validity of MEP (see Figure 5). In TSIC and TSOC paths of **1**, the  $\omega$  value increases steeply after  $\xi \approx -1.5$  and  $-1 \text{ amu}^{1/2}\text{bohr}$ , respectively. They pass through maxima at around  $\xi \approx +1$  and  $+2 \text{ amu}^{1/2}\text{bohr}$  for TSIC and TSOC paths, respectively. After that they gradually decrease as they enter into the stage III. On the other hand, in case of **6**,  $\omega$  value tends to rise sharply from  $\xi \approx -2 \text{ amu}^{1/2}\text{bohr}$  attaining maxima around  $1.6 \text{ amu}^{1/2}\text{bohr}$  in the respective  $\omega$  profiles of TSIC and TSOC paths.

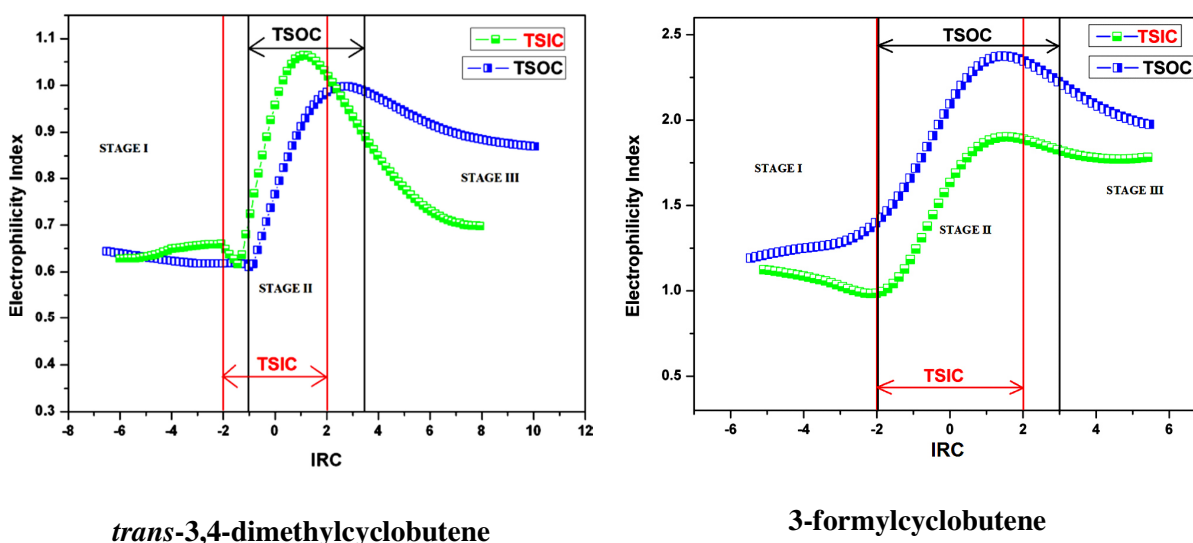


**Figure 5.** Electrophilicity index ( $\omega$ , eV) profiles along IRC ( $\xi$ ,  $\text{amu}^{1/2}\text{bohr}$ ) at the B3LYP/6-31G(d,p) level.

Thereafter, it gradually decreases. Therefore, the maxima in the  $\omega$  profiles lie within the stage II satisfying MEP. In addition, the torquoselective TSOC in **1** and TSIC in **6** are found to be less electrophilic than those of the corresponding unfavorable transition states. Hence, we can say that the complementarity between the MHP and the MEP is met.

In case of the  $\alpha$  profile of **1** along IRC, the maximum occurs at  $\xi \approx +1.5$  amu<sup>1/2</sup>bohr in case of TSIC path and at  $\xi \approx +3.3$  amu<sup>1/2</sup>bohr in case of TSOC path whereas in case of the  $\alpha$  profile of **6** the maxima occur at  $\xi \approx +0.8$  amu<sup>1/2</sup>bohr for both TSOC and TSIC paths (see Figure 6). On the other hand, torquoselective TSOC in **1** and TSIC in **6** are found to be less polarizable than those of other paths. Therefore, we may say that all these three electronic structure principles are obeyed around the TSs, i.e., in stage II region.

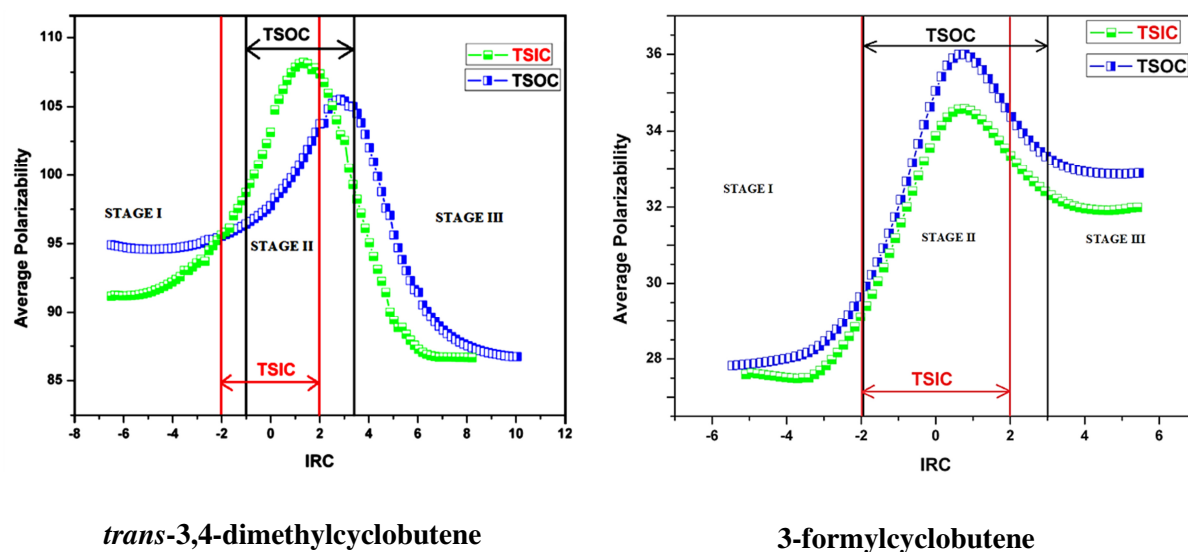


**Figure 6.** Average polarizability ( $\alpha$ , au) profiles along IRC ( $\xi$ , amu<sup>1/2</sup>bohr) at the B3LYP/6-31G(d,p) level.

We have also computed the profiles of local reactivity descriptors like  $f^+$ ,  $f^-$ ,  $\omega^+$  and  $\omega^-$  at C1 and C2 centers of **1** and **6** along IRC. We have chosen C1 and C2 center as these two centers face maximum changes in the structural reorientation. The profiles of  $f^+$  and  $f^-$  at C1 and C2 centers of **1** are provided in Figure 7 whereas those of the  $\omega^+$  and  $\omega^-$  are given in Figure S1 (supporting information). In  $f^+$  profile, the reactivity of both C1 and C2 is almost equivalent at the beginning. However, they pass through an inflection point around TSs. On the other hand, in  $f^-$  profile, the curve for C2 lies somewhat above the curve for C1 in the beginning and then both of the curves go through an inflection point in the stage II, as expected. It may be noted that the inflection points occurred in both the curves for C1 and C2 are almost at the same  $\xi$ . The changes in the reactivity of C1 and C2 centers are major in the stage II. The profiles of  $\omega^+$  and  $\omega^-$

along IRC are almost same as those of  $f^+$  and  $f^-$  so that they also pass through an inflection point around TSs (see Figure S1). Similar observations are obtained in case of **6** (see Figure S2 in supporting information). Therefore, one can locate the region having TSs by following the variation in these local reactivity descriptors along IRC.<sup>50</sup>

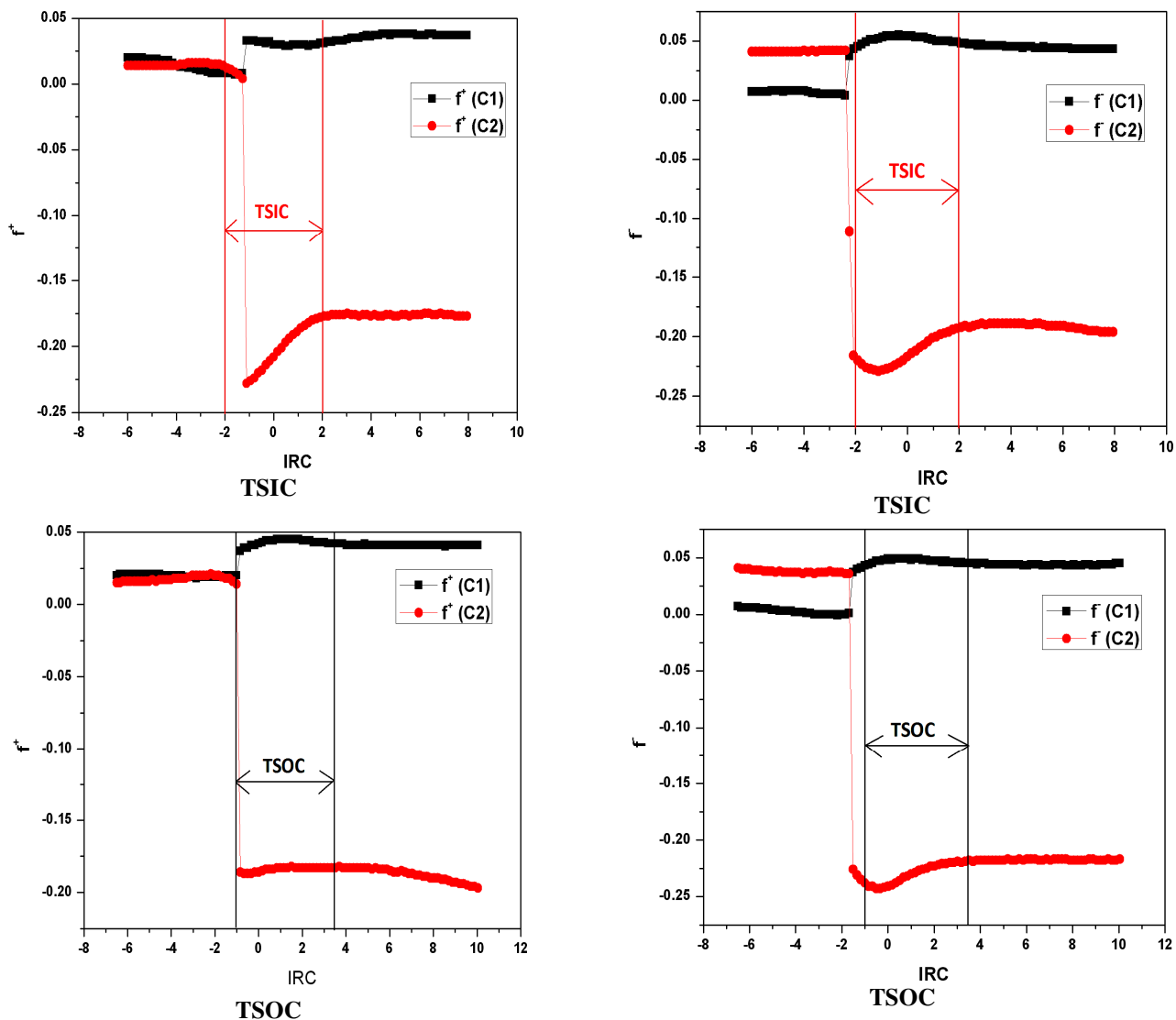


**Figure 7.**  $f^+$  and  $f^-$  (au) profiles at C1 and C2 centers of *trans*-3,4-dimethylcyclobutene along IRC ( $\xi$ ,  $\text{amu}^{1/2}\text{bohr}$ ) at the B3LYP/6-31G(d,p) level.

## Conclusions

In this work, the validity of the maximum hardness (MHP), minimum electrophilicity (MEP) and minimum polarizability principles (MPP) in the torquoselectivity (inward and outward preference) of the conrotatory ring opening reactions of *trans*-3,4-dimethylcyclobutene and 3-formylcyclobutene is evaluated. The reaction profiles are divided into three reaction stages based on the computation of reaction electronic flux along IRC. The regions, where the TSs are located, are identified as  $\xi \approx -2$  to  $+2$  amu<sup>1/2</sup>bohr for TSIC path and at  $\xi \approx -1$  to  $+3.5$  amu<sup>1/2</sup>bohr for TSOC path in case of *trans*-3,4-dimethylcyclobutene and at  $\xi \approx -2$  to  $+2$  amu<sup>1/2</sup>bohr for TSIC path and at  $\xi \approx -2$  to  $+3$  amu<sup>1/2</sup>bohr for TSOC path in case of 3-formylcyclobutene. While the TSIC is found to be higher in energy than that of torquoselective TSOC in *trans*-3,4-dimethylcyclobutene, the TSIC is lower in energy than the unfavorable TSOC in 3-formylcyclobutene. Consequently, the favorable TSOC in *trans*-3,4-dimethylcyclobutene and TSIC in 3-formylcyclobutene are found to be harder, less electrophilic and less polarizable than those of respective unfavorable transition states as expected from the MHP, MEP and MPP. The  $\eta$ ,  $\omega$  and  $\alpha$  profiles along IRC show that the extrema are situated within the region identified as TSs through the reaction electronic flux. The profiles of the local reactivity descriptors ( $f^+$ ,  $f^-$ ,  $\omega^+$ ,  $\omega^-$ ) at C1 and C2 centers along IRC pass through inflection points around the TSs. They are useful in following the reaction path and to identify the region involving TSs.

### Acknowledgments

AMB thanks the Universidad de Talca (CBSM)) for the continuous support to this investigation, through the postdoctoral project N<sup>o</sup> 3150035 (FONDECYT, CHILE) and also Dr. Kendall Houk (University of California, UCLA) for his important comments. PKC thanks DST, New Delhi for the J. C. Bose National Fellowship. SP thanks CSIR, New Delhi for financial assistance.

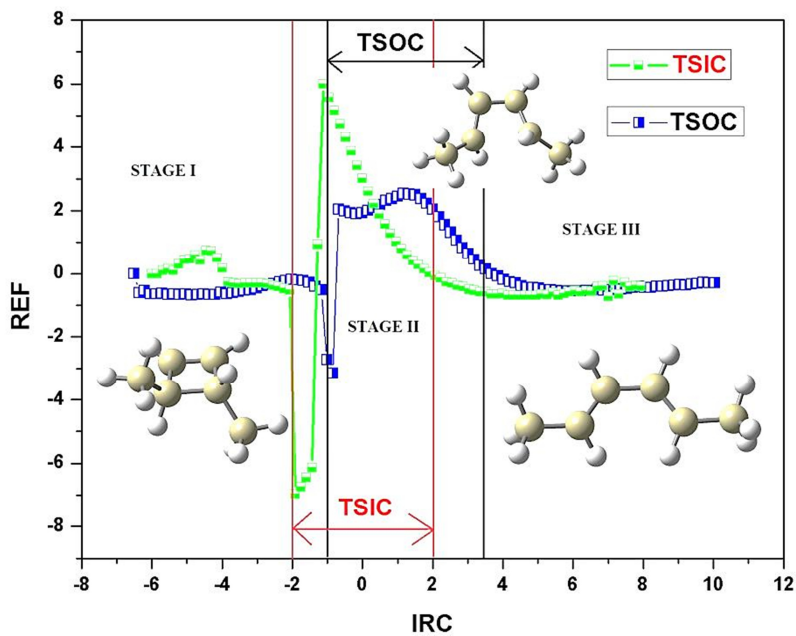
### References

1. R. G. Parr, R. A. Donnelly, M. Levy, and W. E. Palke, *J. Chem. Phys.* 1978, **68**, 3801.

2. J. H. van Vleck The Theory of Electric and Magnetic Susceptibilities, Oxford University Press: Oxford. 1932.
3. R. G. Parr, and R. G. Pearson, *J. Am. Chem. Soc.* 1983, **105**, 7512.
4. R. G. Parr, L. v. Szentpaly, and S. Liu, *J. Am. Chem. Soc.* 1999, **121**, 1922-1924.
5. P. K. Chattaraj, U. Sarkar, and D. R. Roy, *Chem. Rev.* 2006, **106**, 2065-2091.
6. R. G. Pearson, *J. Chem. Educ.* 1987, **64**, 561-567.
7. R. G. Parr, and P. K. Chattaraj, *J. Am. Chem. Soc.* 1991, **113**, 1854-1855.
8. G. Makov, *J. Phys. Chem.* 1995, **99**, 9337-9339.
9. P. K. Chattaraj, P. Pérez, J. Zevallos, and A. Toro-Labbé, *J. Phys. Chem. A* 2001, **105**, 4272-4283.
10. E. Chamorro, P. K. Chattaraj, and P. Fuentealba, *J. Phys. Chem. A* 2003, **107**, 7068-7072.
11. R. Parthasarathi, M. Elango, V. Subramanian, and P. K. Chattaraj, *Theo. Chem. Acc.* 2005, **113**, 257-266.
12. R. G. Parr, and W. Yang, Density functional theory of atoms and molecules, Oxford university press: New York, 1989.
13. P. K. Chattaraj, and S. Sengupta, *J. Phys. Chem.* 1996, **100**, 16126-16130.
14. S. Pan, M. Solá, and P. K. Chattaraj, *J. Phys. Chem A* 2013, **117**, 1843-1852.
15. P. Geerlings, P. W. Ayers, A. Toro-Labbé, P. K. Chattaraj, and F. De Proft, *Acc. Chem. Res.* 2012, **45**, 683-695.
16. W. Kirmse, N. G. Rondan, and K. N. Houk, *J. Am. Chem. Soc.* 1984, **106**, 7989-7991.
17. N. G. Rondan, and K. N. Houk, *J. Am. Chem. Soc.* 1985, **107**, 2099-2111.
18. W. R. Dolbier, K. Koroniak, and K. N. Houk, C. Sheu, *Acc. Chem. Res.* 1996, **29**, 471.
19. A. J. Frontier, and C. Collison, *Tetrahedron* 2005, **61**, 7577-7606.
20. D. R. Timothy, L. M. Morgan, G. H. LeBlanc, R. J. B. Ardagh, and B. Jean, *J. Org. Chem.* 2015, **80**, 1042-1051.
21. H. Banks, *J. Org. Chem.* 2010, **75**, 2510-2517.
22. Y. Takashi, M. Seiji, and S. Mitsuru, *J. Am. Chem. Soc.* 2009, **131**, 2092-2093.
23. J. W. Matthew, N. H. Bruce, E. T. Bert, N. Kensuke, E. A. Kallel, and K. N. Houk, *J. Org. Chem.* 2001, **66**, 6669-6672.
24. C.W. Jefford, G. Bernardinelli, Y. Wang, D. C. Spellmeyer, A. Buda, and K. N. Houk, *J. Am. Chem. Soc.* 1992, **114**, 1157-1165.
25. Y. Naruse, Y. Ichihashi, T. Shimizu, and S. Inagaki, *Org. Lett.* 2012, **14**, 3728-3731.
26. D. J. Kerr, J. Daniel, M. Miletic, J. H. Chaplin, J. M. White, and B. L. Flynn, *Org. Lett.* 2012, **14**, 1732-1735.

27. R. Hayashi, J. B. Feltenberger, and R. P. Hsung, *Org. Lett.* 2010, **12**, 1152-1155.
28. E. A. Kallel, E. Adam, and K. N. Houk, *J. Org. Chem.* 1989, **54**, 6006-6008.
29. B. Buda, Y. Wang, and K. N. Houk, *J. Org. Chem.* 1989, **54**, 2264-2266.
30. K. Rudolf, D. C. Spellmeyer, K. N. Houk, *J. Org. Chem.* 1987, **52**, 3708-3710.
31. S. Niwayama, Y. Wang, K. N. Houk, *Tetrahedron Lett.* 1995, **36**, 6201-6204.
32. K. Nakamura, K. N. Houk, *J. Org. Chem.* 1995, **60**, 686-691.
33. S. Niwayama, E. A. Kallel, D. C. Spellmeyer, C. Sheu, and K. N. Houk *J. Org. Chem.* 1996, **61**, 2813-2825.
34. A. Morales-Bayuelo, *Int. J. Quantum Chem.* 2013, **113**, 1534-1543.
35. A. D. Becke, *Phys. Rev. A* 1998, **38**, 3098-3100.
36. C. Lee, W. Yang, and R. G. Parr, *Phys. Rev. B* 1988, **37**, 785-789.
37. GAUSSIAN 09, Revision C.01, M. J. Frisch et al., Gaussian, Inc., Wallingford CT. 2010.
38. P. Geerlings, F. De Proft, and W. Langenaeker, *Chem. Rev.* 2003, **103**, 1793-1873.
39. S. B. Liu, *Acta Phys.-Chim. Sin.* 2009, **25**, 590 - 600.
40. Chemical Reactivity Theory: A Density Functional View, ed. P. K. Chattaraj, Taylor & Francis/CRC Press, Florida, 2009.
41. R. G. Parr, and W. Yang, *J. Am. Chem. Soc.* 1984, **106**, 4049-4050.
42. W. Yang, and W. J. Mortier, *J. Am. Chem. Soc.* 1986, **108**, 5708-5711.
43. P. K. Chattaraj, B. Maiti, and U. Sarkar, *J. Phys. Chem. A* 2003, **107**, 4973-4975.
44. D. R. Roy, R. Parthasarathi, J. Padmanabhan, U. Sarkar, V. Subramanian, and P. K. Chattaraj, *J. Phys. Chem. A* 2006, **110**, 1084-1093.
45. B. Herrera, and A. Toro-Labbé, *J. Phys. Chem. A* 2007, **111**, 5921-5926.
46. IUPAC, Compendium of Chemical Terminology, 2nd ed. (the "Gold Book") (1997). Online corrected version: (2006-) "transition state theory".
47. K. J. Laidler, Chemical kinetics, Pearson Education Inc. Third edition, ISBN 978-81-317-0972-6.
48. J. C. Polanyi, and A. H. Zewail, *Acc. Chem. Res.* 1995, **28**, 119-132.
49. A. H. Zewail, *J. Phys. Chem. A* 2000, **104**, 5660-5696.
50. P. K. Chattaraj, and D. R. Roy, *J. Phys. Chem. A* 2006, **110**, 11401-11403.

## Graphical Abstract



The phenomenon of the torquoselectivity in the electrocyclic ring opening reactions is explained through the electronic structure principles.